Monthly Notices of the ROYAL ASTRONOMICAL SOCIETY
MNRAS **480,** 2939–2944 (2018) doi:10.1093/mnras/sty2018
Advance Access publication 2018 July 27

The magnetic field structure in molecular cloud filaments

Gilberto C. Gómez,[1★] Enrique Vázquez-Semadeni[1] and Manuel Zamora-Avilés[1,2]

[1] *Instituto de Radioastronomía y Astrofísica, Universidad Nacional Autónoma de México, Apdo. postal 3-72, Morelia Mich. 58089, México*
[2] *Department of Astronomy, University of Michigan, 500 Church Street, Ann Arbor, MI 48105, USA*

Accepted 2018 July 20. Received 2018 June 29; in original form 2018 January 9

ABSTRACT

We explore the structure of magnetic field lines in and around filaments in simulations of molecular clouds undergoing global, multiscale gravitational collapse. In these simulations, filaments are not in a static equilibrium, but are long-lived flow structures that accrete gas from their environment and direct it towards clumps embedded in the filament or at the nodes at the conjunction with other filaments. In this context, the magnetic field is dragged by the collapsing gas, so its structure must reflect the flow that generates the filament. Around the filament, the gas is accreted on to it, and the magnetic lines must then be perpendicular to the filament. As the gas density increases, the gas flow changes direction, becoming almost parallel to the filament, and magnetic lines also tend to align with it. At the spine of the filament, however, magnetic lines become perpendicular again since they must connect to lines on the opposite side of the filament, resulting in 'U'-shaped magnetic structures, which tend to be stretched by the longitudinal flow along the filament. Magnetic diffusive processes, however, allow the gas to continue to flow. Assuming a stationary state in which the ram pressure of the flow balances the magnetic tension, the curvature of the field lines is determined by the diffusion rate. We derive an expression relating the curvature of the field lines to the diffusive coefficient, which may be used to observationally determine the nature of the diffusive process.

Key words: MHD – ISM: clouds – ISM: kinematics and dynamics – ISM: magnetic fields.

1 INTRODUCTION

The ubiquity of filaments in molecular clouds has been clearly established by numerous infrared continuum and molecular line observations (Bally et al. 1987; Myers 2009; André et al. 2010; Molinari et al. 2010; Arzoumanian et al. 2011; Kirk et al. 2013; Palmeirim et al. 2013; Peretto et al. 2014; Li et al. 2016; Rivera-Ingraham et al. 2016). However, the internal structure and kinematics of the filaments are still debated. A class of published models assumes that the filaments are in hydrostatic equilibrium (e.g. Stodółkiewicz 1963; Ostriker 1964; Inutsuka & Miyama 1992; Fischera & Martin 2012; Burge et al. 2016), but this leaves open the question of how the filaments were formed in the first place and how they reached such an equilibrium. Another proposed model assumes that the filaments form as a consequence of turbulent compressions in the clouds (e.g. Padoan et al. 2001; Auddy, Basu & Kudoh 2016). Finally, yet another class of models assumes that the filaments form as part of the global gravitational collapse of a molecular cloud as a whole, and therefore the filaments radially accrete material from their parent clouds (Heitsch 2013a,b; Hennebelle & André 2013). However, neither of these models accounts for the observation that the gas appears to be flowing along the filaments towards the cores and 'hubs' located within the filaments (e.g. Schneider et al. 2010; Sugitani et al. 2011; Kirk et al. 2013; Peretto et al. 2014).

Balsara, Ward-Thompson & Crutcher (2001), based in MHD simulations of gravitationally collapsing clouds, proposed that filaments accrete gas towards the cores formed at the filaments' intersections. Those authors suggested that such a flow is directed by magnetic flux tubes along the filaments. A different scenario was proposed by Gómez & Vázquez-Semadeni (2014, hereafter GV14; see also Smith et al. 2016). In their simulations without a magnetic field, filaments developed self-consistently as a consequence of the gravitational collapse only. Similarly to Balsara et al. (2001), GV14 suggested that the filaments are flow structures, accreting gas from the cloud and redirecting it towards the star-forming clumps that are formed both within the filaments and at their intersections with other filaments. In this picture, the filaments are out-of-equilibrium, river-like structures, along which the gas from a cloud flows down the gravitational potential towards a clump located at the potential minimum. The filament is, simply, the locus of this flow along a local trough in the potential. In this scenario, the filaments arise from the strongly anisotropic global collapse of the cloud, which naturally forms sheets and filaments (Lin, Mestel & Shu 1965), growing from small perturbations, and then reaching approximately stationary regimes for as long as the gas supply from the cloud remains (GV14). Thus, their growth and observed dynamical nature are nat-

★ E-mail: g.gomez@irya.unam.mx

urally explained. It is important to remark that the flow observed by GV14 along the filaments did not develop internal shocks nor strong turbulence, the flow being relatively laminar.

Magnetic fields have also been observed associated with molecular clouds and embedded filaments, often appearing roughly perpendicular to the filaments (e.g. Goodman et al. 1992; Chapman et al. 2011; Palmeirim et al. 2013; Planck Collaboration XXXV 2016). Numerical simulations have also shown that filaments form preferably perpendicular to magnetic field lines (e.g. Hennebelle 2013; Zamora-Avilés, Ballesteros-Paredes & Hartmann 2017). Their impact in the molecular cloud formation and evolution is still a subject of debate, although a frequent interpretation is that the magnetic field is somehow responsible for the formation of the filament, by allowing the gas to flow towards it. However, this interpretation does not provide an answer to the question of what is driving the gas to flow along the field towards the filament. In this regard, Vázquez-Semadeni et al. (2011) presented simulations of cloud formation in the colliding flow scenario in the presence of self-gravity and magnetic fields oriented parallel to the colliding flows. These simulations showed that the evolution is similar to that of the non-magnetic case, because the cloud increases its mass-to-flux ratio (M2FR) by accretion along the field lines, eventually becoming magnetically supercritical and proceeding to global collapse. The cloud in those simulations consists of high-density, high-M2FR clumps surrounded by low-density, low-M2FR bubbles. These low-density bubbles are buoyant and allow the dense clumps to percolate to the centre of the cloud 'through a process that appears as the macroscopic-scale analogue of AD (ambipolar diffusion) ... so that the clouds evolve towards a segregated state with low M2FR in their periphery and high M2FR towards their centre' (Vázquez-Semadeni et al. 2011).

Since the evolution of the cloud presented in Vázquez-Semadeni et al. (2011) is similar to that observed in non-magnetic simulations of molecular cloud formation, including the formation of filaments (e.g. Vázquez-Semadeni et al. 2007; Heitsch & Hartmann 2008), it is necessary to determine whether the filaments formed in magnetized simulations also behave as the flow structures mentioned earlier and, if so, how is the magnetic field affected by the accretion towards and along a filament formed in a cloud undergoing global gravitational collapse. In this contribution we explore this question in one of the MHD simulations presented by Zamora-Avilés et al. (2018). In Section 2, we briefly describe the simulation. In Section 3, we discuss the resulting magnetic field structure associated with the flow around a filament in the simulation. In Section 4, we discuss how the magnetic field geometry may be used to explore the dominant diffusive process in the medium. Finally, in Section 5, we summarize our conclusions.

2 THE NUMERICAL MODEL

The filament studied here comes from the MHD simulation presented in Zamora-Avilés et al. (2018) labelled B3J, which is aimed at studying the effect of magnetic fields on the production of turbulence through various instabilities during the formation of MCs by converging flows and the subsequent star formation activity. It was performed using the Eulerian adaptive mesh refinement FLASH (v2.5) code (Fryxell et al. 2000) to obtain three-dimensional, self-gravitating, ideal-MHD simulations, including heating and cooling processes, and a Jeans refinement criterion. For more details, we refer the reader to Zamora-Avilés et al. (2018).

In this simulation, the numerical box, of dimensions $L_x = 256$ pc and $L_y = L_z = 128$ pc, is initially filled with warm neutral gas at a uniform density $n = 2\,\mathrm{cm}^{-3}$ (with a mean molecular weight $\mu = 1.27$) and a constant temperature of 1450 K, which corresponds to thermal equilibrium. The initial velocity field contains turbulent fluctuations with a Burger's type spectrum corresponding to an rms Mach number of 0.7 (with respect to the isothermal sound speed of $3.0\,\mathrm{km\,s}^{-1}$). On top of this turbulent field, we add two cylindrical streams, each of radius $R_{\mathrm{inf}} = 32$ pc and length $L_{\mathrm{inf}} = 112$ pc along the x-direction, moving in opposite directions at a moderately supersonic velocity of $7.5\,\mathrm{km\,s}^{-1}$.

The numerical box is permeated with an initially uniform magnetic field of 3μG parallel to the inflows.[1] Unlike the simulations by Zamora-Avilés et al. (2018) (which have a maximum resolution of $\Delta x = 3.1 \times 10^{-2}$ pc), here we allow the simulation to refine eight levels more to reach a maximum resolution of 1.2×10^{-4} pc. The corresponding sink formation density threshold is $n_{\mathrm{thr}} = 2.1 \times 10^9\,\mathrm{cm}^{-3}$.

Although it has been stated that a magnetic field perpendicular to the inflows (i.e. parallel to the shock surface) may inhibit the formation of a cloud (Inoue & Inutsuka 2009), we consider such a configuration as unlikely to happen in reality. The colliding flow scenario used here is thought to be a representative of the gas flow in and around spiral arms, where magnetic field is parallel to the large-scale gas flow (see for example, fig. 8 in Gómez & Cox 2004).

3 MAGNETIC FIELD STRUCTURE

As described in GV14, as the cloud collapses as a whole, filaments are formed in the regions where the gas accretion turns from two-dimensional (sheet-like accretion to the filaments from their environment) to one-dimensional (along the filaments to cores). This accretion occurs where the magnetic field is weaker and, therefore, it is dragged by the gas flow. A simple picture of the resulting magnetic field line geometry is presented in Fig. 1. Around the filament, the magnetic field must be mainly perpendicular to the filament since the accretion flow has that direction. As the gas velocity turns and the flow becomes dominated by the longitudinal motion along the filament, the magnetic lines must also develop a component parallel to the filament. At some point, the magnetic lines must turn back and connect with the (perpendicular) lines on the other side of the filament. So, at the filament spine, the magnetic field must be perpendicular to the filament again, resulting in a 'U'-shaped magnetic line across the filament: perpendicular in the surroundings, then oblique, and perpendicular again in the centre. Of course, in this high-density region the increasing magnetic tension and the opposite magnetic polarities must play a role, either through magnetic reconnection or AD (Section 4. See also Hennebelle & André 2013).

Fig. 2 shows a filament of the simulation. Colours show the column density of gas, while the 'drapery' pattern indicates the direction of the (density-weighted) mean magnetic field. The above described 'U'-shaped magnetic lines associated with the filament are clearly visible in the vertical segment at $(z, y) \approx (-9.5, 7)$ pc and the slanted segment at $(z, y) \approx (-9, 6)$ pc. They are also visible, although not as clearly, in the segment near the top of the filament, at $(z, y) \approx (-9.5, 8)$ pc. Note that near the bottom of the filament, at $(z, y) \approx (-9, 6)$ pc, the 'U'-shaped lines appear to point away from the embedded clump. This does not contradict the above

[1]Note that the corresponding mass-to-flux ratio is 1.59 times greater than the critical value, $\mu_{\mathrm{crit}} = 0.16/\sqrt{G}$ (Nakano & Nakamura 1978), so that our entire numerical box is magnetically supercritical.

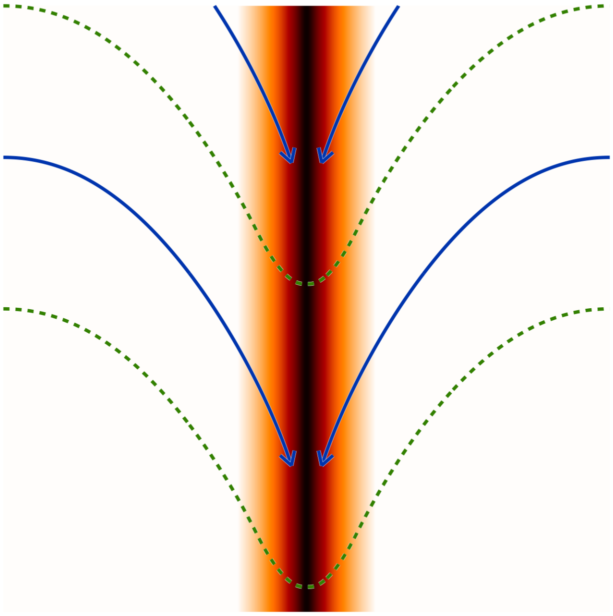

Figure 1. Simplified picture of the 'U'-shaped magnetic line geometry due to the accretion towards and along the filament. Colours indicate the projected column density of the filament, while the solid lines show the flow of gas and the dashed lines show the magnetic field lines, dragged by the accretion flow. The filament column density profile and the velocity field are an approximation to the fits presented in GV14.

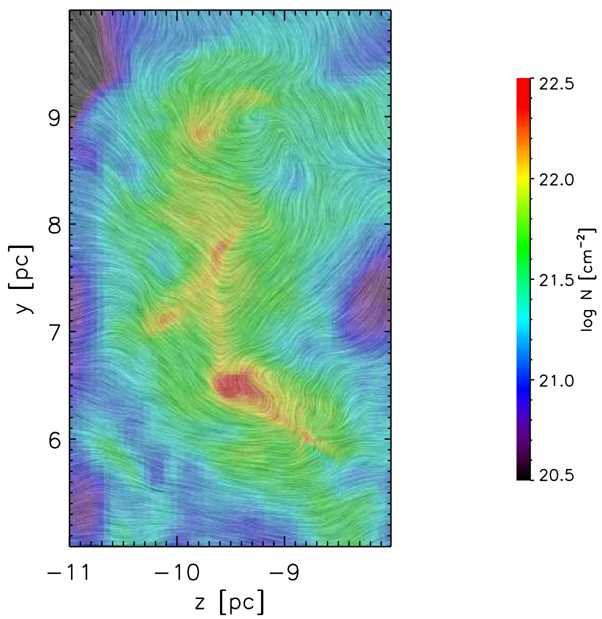

Figure 2. Column density of a filament with its magnetic field direction, 13.1 Myr after the beginning of the simulation. Coordinates are with respect to the centre of the simulation box. The overlaid 'drapery' pattern represents the (density-weighted) mean magnetic field in the z–y plane, visualized using the line-integral-convolution technique (Cabral & Leedom 1993). The 'U'-shaped magnetic structures due to the gas accretion are apparent.

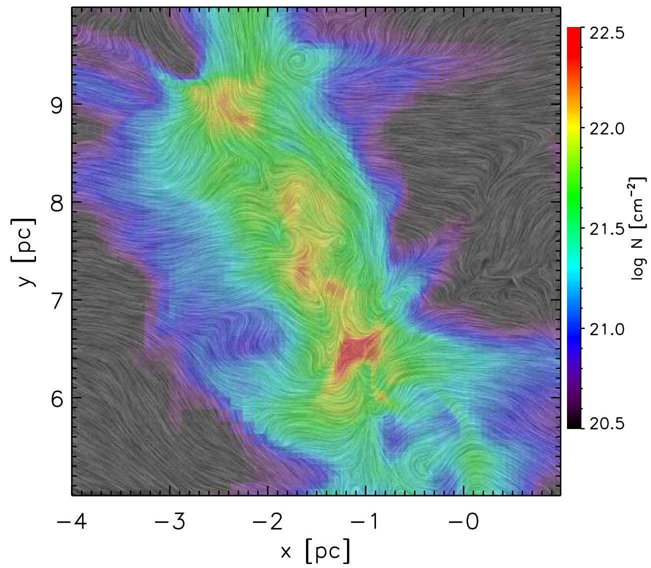

Figure 3. Same region as in Fig. 2, but with column density and mean magnetic field integrated along the z-direction. In contrast with that figure, the 'U'-shaped magnetic structures are not visible.

described picture since the molecular cloud as a whole is experiencing gravitational collapse, so that the material in the filament is flowing towards a collapse centre located outside of the region shown in the figure. Nevertheless, as discussed in GV14, secondary collapses do occur within the filament itself, generating a velocity gradient along the filament. This is seen in Fig. 2 to cause different degrees of curvature of the magnetic field lines at different parts of the filament. Therefore, the structures contained within the cloud also drag the magnetic field and generate magnetic 'U'-structures associated with this large-scale flow.

Obviously, the scenario described in Fig. 1 is an idealized one and an axisymmetric version would be difficult to achieve. As an example, Fig. 3 shows another projection of the same filament. In this case, the 'U'-shaped structures are not as clear as in the Fig. 2. A possible reason for this is the following: The near-pressureless collapse of a molecular cloud means that density structures collapse along the shortest dimension first, going from a (three-dimensional) ellipsoid to a (two-dimensional) sheet and further to a (one-dimensional) filament. So, the accretion towards the filament will not be axisymmetric, but from a planar environment. In this scenario, it is not surprising that the magnetic field lines, dragged by the flow, will adopt a geometry that reflects this dimensionality of the accretion flow. So, the 'U'-shaped magnetic lines associated with the filaments might be observable along some directions only, but their absence may not be considered as evidence of absence of flow along the filament.

3.1 Filament evolution

Fig. 4 shows the time evolution of the filament along 5.6 Myr. The now familiar 'U'-shaped magnetic structures are visible before the filament is apparent in density (panel *a*) since, on the one hand, the compressive flow that originates the filament must predate it, and on the other, the cloud as a whole is already undergoing global collapse, while at the same time some collapse centres are already present, as filaments and cores are observed to form simultaneously in the simulations (Camacho et al. 2016). Therefore, the accretion

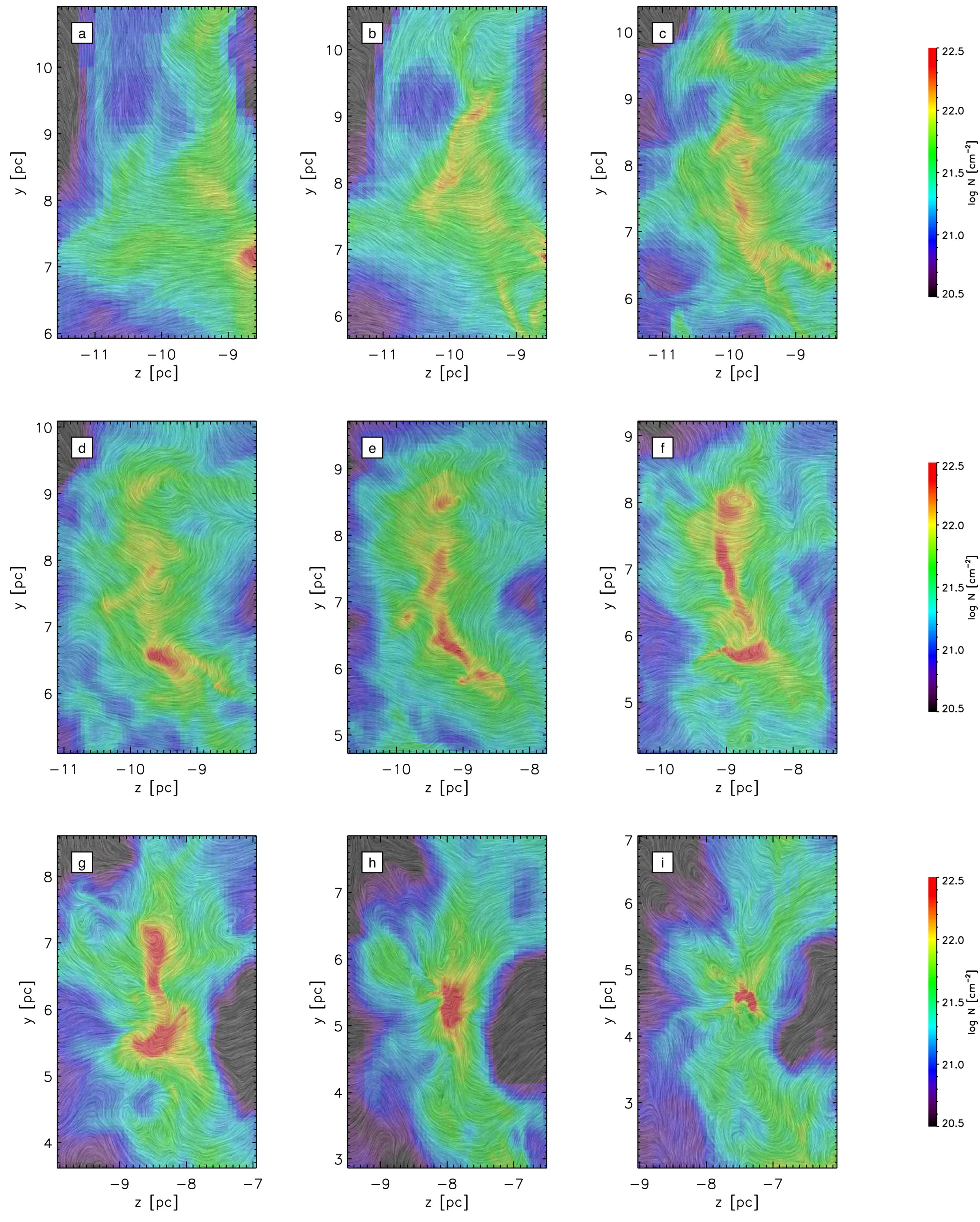

Figure 4. Evolution of the filament and its associated magnetic structure. Times shown correspond to 10.8 (panel *a*) through 16.4 Myr (panel *i*) from the start of the simulation, in 0.7 Myr increments. Although all panels show regions of the same size, their positions in the simulation box change in order to follow the evolution of the filament as it moves following the large-scale gravitational collapse.

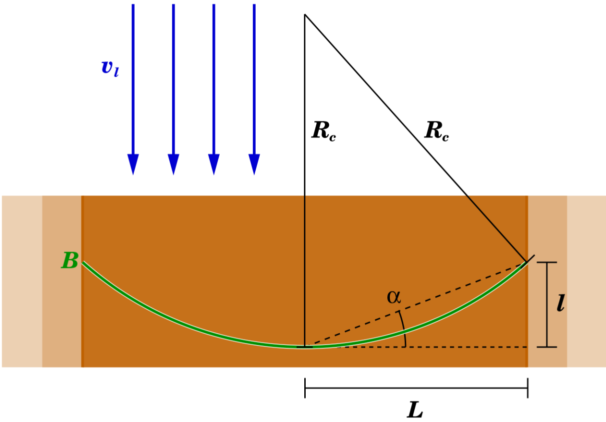

Figure 5. Schematic for the ram-pressure bending of magnetic field lines (see Section 4). The gas flows with velocity v_l within the filament's core, of radius L. The force exerted by this flow drags the magnetic line a distance l and inducing a curvature of radius R_c.

towards the (future) filament and towards the embedded core is already happening and so it should drag the magnetic field with it.

These broad initial 'U'-structures become narrower as the filament's density increases and the accretion flow becomes better defined. Eventually, smaller collapse centres appear within the filament (as described in GV14), leading to a more complex velocity and magnetic structure. 14.3 Myr into the simulation (panel *f*), the filament-core self-gravity starts to dominate the small-scale evolution and, while the filament as a whole keeps falling into the cloud's centre, it rapidly collapses longitudinally. This is reflected in less prominent large-scale 'U'-shaped structures (although some are still visible near the larger cores). At 16.4 Myr (panel *i*), the filament as a whole collapses into a large core, with some low-column density structures remaining in the surroundings. By this time, stellar feedback (not included in this simulation) should have an impact on the low-density gas around the core (Colín, Vázquez-Semadeni & Gómez 2013; see also Körtgen et al. 2016), and so this stage of the filament's evolution becomes less reliable.

4 MAGNETIC DIFFUSION

As the gas flows along the centre of the filament drag the magnetic field, the increasing curvature of the 'U'-shaped lines means that the magnetic forces can no longer be dismissed. If we assume that diffusion effects separate the gas flow from the magnetic field lines, we may connect observables with the characteristics of the flow along the filament or with the parameters of the diffusion process at work.

Consider the simple picture of the filament and associated magnetic lines shown in Fig. 5. At the filament's spine, the shape of the magnetic line will be defined by a balance between magnetic tension and the ram pressure due to the flow along the filament:

$$\frac{\rho v_A^2}{R_c} = \frac{\rho v_l^2}{2L}, \tag{1}$$

where ρ is the gas density, v_A is the Alfvén velocity, R_c is the line curvature, v_l is the gas velocity along the filament, and L is the filament half-width. If $R_c > L$, we may rewrite equation (1) in terms of easier-to-measure quantities. Let l be the depth of the 'U'-shaped line along the filament. Then, the angle between the magnetic line and the direction perpendicular to the filament, α, is related to the above defined lengths by $\tan(\alpha) = l/L$. In turn, l is related to the curvature radius by $R_c^2 = (R_c - l)^2 + L^2$. Simple algebraic manipulation leads to $R_c = L/\sin(2\alpha)$, and thus equation (1) becomes

$$\left(\frac{v_l}{v_A}\right)^2 = 2\sin(2\alpha). \tag{2}$$

The physics of the diffusive process is reflected in the length the gas moves before the magnetic field decouples from the flow, so $l = v_l \tau_{\rm dif}$, where $\tau_{\rm dif}$ is the diffusion time-scale. Then, we may use the observables α, L, v_l, and v_A to estimate $\tau_{\rm dif}$ and so explore the magnetic diffusion process at hand. For example, for the point at $(x, y, z) = (-1.2, 6.2, -8.7)$ pc at $t = 14.3$ Myr, which is located in a filament flowing into the lower clump visible in Fig. 4(f), the magnetic line deformation ($l \sim 0.32$ pc) and the flow speed along the filament ($v_l \sim 1.19$ km s^{-1}) imply a diffusive time-scale $\tau_{\rm dif} = l/v_l \sim 0.26$ Myr. This can be compared to the characteristic time-scale of known diffusive processes, such as linear and turbulent AD (Mestel & Spitzer 1956; Mouschovias 1991; Heitsch et al. 2004), as well as reconnection diffusion (Lazarian & Vishniac 1999).

For the case of linear AD, noting that the gas density at the above quoted point is 8.43×10^3 cm^{-3}, the Alfvén velocity is 0.12 km s^{-1}, and the filament half-width is $L = 0.088$ pc, the characteristic time-scale is $\tau_{\rm dif,amb} = 107$ Myr (see equation 13 in Hennebelle & André 2013). Clearly, the linear AD time-scale is much larger than the observed diffusion scale. This is not surprising, as this process is known to be very slow, and various suggestions have been made to allow it to act on shorter time-scales (e.g. Ciolek & Basu 2001; Heitsch et al. 2004).

Concerning reconnection diffusion, the magnetic field diffusion in our simulation must be of numerical origin, since no explicit diffusive terms are included in the equations solved. However, Lazarian & Vishniac (1999) and Kowal et al. (2009) have argued that the reconnection rate is independent of the resistivity, and Santos-Lima, de Gouveia Dal Pino & Lazarian (2012) have used this fact to rely on numerical resistivity to estimate the effects of reconnection diffusion. Under this assumption, the diffusion time-scale we have estimated above should coincide with the reconnection diffusion time-scale. However, given the values of the flow speed and the Alfvén speed above, we note that the flow along the filament is strongly super-Alfvénic, and Kim & Diamond (2001) and Lazarian et al. (2015) have argued that the reconnection speed derived by Lazarian & Vishniac (1999) fails for super-Alfvénic cases. We thus defer a comparison of our diffusion time-scale with the predictions of reconnection diffusion in this system to a later contribution. We also defer a comparison with turbulent AD since this involves a detailed study of the ratio of magnetic and turbulent kinetic energies as a function of scale.

5 DISCUSSION

Observations of magnetic fields in molecular cloud filaments show that the field is perpendicular to the filaments in the surrounding and central regions (Goodman et al. 1992; Palmeirim et al. 2013). This geometry is usually interpreted as the field being perpendicular to the filament, which is then taken as evidence for the flow being dominated by the field (Sugitani et al. 2011; Li et al. 2013). The picture described in this article, in which the flow is dominated by gas accretion and the field is dragged with the flow, is not inconsistent with the observations, since the magnetic field is harder to observe in the intermediate-density regions where the lines turn and become aligned by the flow with the filament. Observational resolution, or lack thereof, would lead to less pronounced observed 'U'-shaped lines, in addition to a lower degree of polarization in the emission. We will explore this observational effect in a future work.

Magnetic structures qualitatively similar to the ones described here are visible in the Planck maps of magnetic fields associated with molecular clouds. For example, fig. 1 in Planck Collaboration XXXV (2016) shows the column density and magnetic field direction towards the Taurus molecular cloud. At galactic coordinates (l, b) $\sim$ (168°, 16.2°), the magnetic field lines follow the 'U'-shape we associate with the accretion flow around and along a filament in a globally collapsing cloud. Further left in the same figure, the magnetic lines are still bent for some 4° along galactic longitude. Although the reader should keep in mind that the physical scales in the Taurus filaments and our simulation are quite different, the similarity of that figure and our Fig. 5(e) is striking and it is easy to speculate if a similar mechanism is at work. Curved magnetic fields have also been observed in the main filament of Serpens South, which have been associated with gravitational contraction along the filament (Sugitani et al. 2011).

An important assumption for this work is that the gas dynamics of the collapsing cloud is dominated by self-gravity, and so the evolution might be considered pressureless. Vázquez-Semadeni et al. (2011) showed that the magnetically subcritical regions percolate away from the cloud, thus allowing for the collapse of the supercritical regions, so the presence of a magnetic field should not alter significantly the large-scale evolution of the cloud. In the picture presented here, the gas accretion flow along the filament will be affected by the magnetic tension in the dense central regions of the filament, since the 'U'-shaped lines counteract the gravitational flow towards the collapsing regions embedded within the filaments until the magnetic diffusion allows the flow to continue. Thus, the accretion along the filament which feeds the star-forming cores will be connected to the details of the diffusive process happening in the central regions of the filaments. Since AD is too slow to play an important part in the filament dynamics, reconnection diffusion (Lazarian & Vishniac 1999) and turbulent AD (Heitsch et al. 2004) appear to be interesting possibilities to separate the gas flow from magnetic stresses. Since this reconnection is related to the turbulent characteristics of the fluid, the study of 'U'-shaped magnetic field lines might be useful to study the nature of unresolved motions in the central parts of molecular filaments.

ACKNOWLEDGEMENTS

We thank B. Bukhart, A. Lazarian, S. Lizano, I. Ristorcelli, and J. Soler for useful comments during the development of this project. We also thank an anonymous referee for reviewing this manuscript. This work received financial support from UNAM-DGAPA PAPIIT grant IN100916 to GCG and CONACyT grant 255295 to EVS. MZA acknowledges CONACyT for a postdoctoral fellowship at University of Michigan. The FLASH code used in this work was in part developed by the DOE NNSA-ASC OASCR Flash Center at the University of Chicago.

REFERENCES

André P. et al., 2010, A&A, 518, L102
Arzoumanian D. et al., 2011, A&A, 529, L6
Auddy S., Basu S., Kudoh T., 2016, ApJ, 831, 46
Bally J., Lanber W. D., Stark A. A., Wilson R. W., 1987, ApJ, 312, L45
Balsara D., Ward-Thompson D., Crutcher R. M., 2001, MNRAS, 327, 715
Burge C. A., Van Loo S., Falle S. A. E. G., Hartquist T. W., 2016, A&A, 596, A28
Cabral B., Leedom L. C., 1993, SIGGRAPH '93 Proceedings of the 20th Annual Conference on Computer Graphics and Interactive Techniques, Imaging Vector Fields Using Line Integral Convolution. ACM, New York, NY, p. 263
Camacho V., Vázquez-Semadeni E., Ballesteros-Paredes J., Gómez G. C., Fall S. M., Mata-Chávez M. D., 2016, ApJ, 833, 113
Chapman N. L., Goldsmith P. F., Pineda J. L., Clemens D. P., Li D., Krčo M., 2011, ApJ, 741, 21
Ciolek G. E., Basu S., 2001, ApJ, 547, 272
Colín P., Vázquez-Semadeni E., Gómez G. C., 2013, MNRAS, 435, 1701
Fischera J., Martin P., 2012, A&A, 542, A77
Fryxell B. et al., 2000, ApJS, 131, 273
Gómez G. C., Cox D. P., 2004, ApJ, 615, 744
Gómez G. C., Vázquez-Semadeni E., 2014, ApJ, 791, 124 (GV14)
Goodman A. A., Jones T. J., Lada E. A., Myers P. C., 1992, ApJ, 399, 108
Heitsch F., 2013a, ApJ, 769, 115
Heitsch F., 2013b, ApJ, 776, 62
Heitsch F., Hartmann L., 2008, ApJ, 689, 290
Heitsch F., Zweibel E., Slyz A., Devriendt J., 2004, ApJ, 603, 165
Hennebelle P., 2013, A&A, 556, A153
Hennebelle P., André P., 2013, A&A, 560, A68
Inoue T., Inutsuka S., 2009, ApJ, 704, 161
Inutsuka S.-I., Miyama S. M., 1992, ApJ, 388, 392
Kim E.-j., Diamond P. H., 2001, ApJ, 556, 1052
Kirk H., Myers P. C., Bourke T. L., Gutermuth R. A., Hedden A., Wilson G. W., 2013, ApJ, 766, 115
Körtgen B., Seifried D., Banerjee R., Vázquez-Semadeni E., Zamora-Avilés M., 2016, MNRAS, 459, 3460
Kowal G., Lazarian A., Vishniac E. T., Otmianowska-Mazur K., 2009, ApJ, 700, 63
Lazarian A., Vishniac E. T., 1999, ApJ, 517, 700
Lazarian A., Eyink G., Vishniac E., Kowal G., 2015, Phil. Trans. R. Soc. London Ser. A, 373, 20140144
Li H., Fang M., Henning T., Kainulainen J., 2013, MNRAS, 436, 3707
Li G., Urquhart J., Leurini. S., Csengeri T., Wyrowski F., Menten K. M., Schuller F., 2016, A&A, 591, A5
Lin C. C., Mestel L., Shu F. H., 1965, ApJ, 142, 1431
Mestel L., Spitzer L., 1956, MNRAS, 116, 503
Molinari S. et al., 2010, A&A, 518, L100
Mouschovias T. C., 1991, in Lada C. J., Kylafis N. D., eds, Proc. NATO ASIC 342, The Physics of Star Formation and Early Stellar Evolution. Kluwer, Dordrecht, p. 449
Myers P. C., 2009, ApJ, 700, 1609
Nakano T., Nakamura T., 1978, PASJ, 30, 671
Ostriker J., 1964, ApJ, 140, 1056
Padoan P., Juvela M., Goodman A. A., Nordlund Å., 2001, ApJ, 553, 227
Palmeirim P. et al., 2013, A&A, 550, A38
Peretto N. et al., 2014, A&A, 561, A83
Planck Collaboration XXXV, 2016, A&A, 586, A138
Rivera-Ingraham A. et al., 2016, A&A, 591, A90
Santos-Lima R., de Gouveia Dal Pino E. M., Lazarian A., 2012, ApJ, 747, 21
Schneider N., Csengeri T., Bontemps S., Motte F., Simon R., Hennebelle P., Federrath C., Klessen R., 2010, A&A, 520, A49
Smith R. J., Glover S. C. O., Klessen R. S., Fuller G. A., 2016, MNRAS, 455, 3640
Stodółkiewicz J. S., 1963, Acta Astron., 13, 30
Sugitani K. et al., 2011, ApJ, 734, 63
Vázquez-Semadeni E., Gómez G. C., Jappsen A. K., Ballesteros-Paredes J., González R. F., Klessen R. S., 2007, ApJ, 657, 870
Vázquez-Semadeni E., Banerjee R., Gómez G. C., Hennebelle P., Duffin D., Klessen R. S., 2011, MNRAS, 414, 2511
Zamora-Avilés M., Ballesteros-Paredes J., Hartmann L. W., 2017, MNRAS, 472, 647
Zamora-Avilés M., Vázquez-Semadeni E., Körtgen B., Banerjee R., Hartmann L., 2018, MNRAS, 474, 4824

This paper has been typeset from a TEX/LATEX file prepared by the author.